Available online at www.sciencedirect.com

ScienceDirect

Advances in Space Research 66 (2020) 2319–2337

ADVANCES IN SPACE RESEARCH (a COSPAR publication)

www.elsevier.com/locate/asr

Calibration and verification of century based wave climate data record along the Turkish coasts using satellite altimeter data

B. Oztunali Ozbahceci [a,*], A.R. Turgut [a], A. Bozoklu [a], S. Abdalla [b]

[a] Izmir Institute of Technology, Civil Engineering Department, Gulbahce, 35430 Urla, Izmir, Turkey
[b] ECMWF, Shinfield Park, RG2 9AX Reading, UK

Received 11 June 2019; received in revised form 23 January 2020; accepted 15 February 2020
Available online 26 February 2020

Abstract

In order to produce consistent reanalysis of the climate system, ECMWF (The European Centre for Medium-Range Weather Forecasts) has produced firstly an uncoupled atmospheric reanalysis ERA-20C, and then a coupled climate reanalysis, called CERA-20C, which covers the period January 1900 to December 2010. Both data sets are available at 3-hour time increments. Such a century long data can be an alternative to calculate the extreme waves corresponding to low probability of occurrences without extrapolation of extreme value statistics' results which may contribute to the error in the estimation of design waves in case of small number of wave data. In this study, main purpose is to calibrate and verify the century-based wave data in order to derive the longest and the consistent wave data along the Turkish coasts as a first time to be used in the extreme wave analysis. For this purpose, first of all, significant wave height data of ERA-20C and CERA-20C are compared by using ENVISAT data over the whole Black Sea for 2007–2008 as a pilot study. Comparison results show that both datasets give similar results but CERA-20C seems to be better in terms of statistical error measures. Then CERA-20C significant wave height data are calibrated using satellite Radar Altimeter data set. Jason family of satellites (TOPEX, Jason-1 and 2) and Envisat family of satellites (ERS-2 and Envisat) are inter-calibrated to get the consistent satellite data sets with a total duration of 18 years (1995–2012) for Envisat family and 26 years (1992–2017) for Jason family in order to be used in calibration of CERA-20C wave height. The mean wave period is also estimated from RA backscatter coefficients (Ku and C bands) and the significant wave height by using Artificial Neural Network Method. Then the estimated mean wave periods are used for the calibration of CERA-20C wave period. Calibrated CERA-20C data are compared with in-situ measurements for the verification purposes. Results of verification study show that the calibrated CERA-20C wave data agree well with the in-situ measurements in terms of Quantile-Quantile analysis with lower deviations from y = x line and capture the largest sea states. In fact, CERA-20C, century-based wave data become appropriate to determine the extreme waves to be used in the design of coastal structures along the Turkish coasts.

Keywords: Wave climate; Extreme wave; CERA-20C; Radar altimeter; Significant wave height; Mean wave period; ANN; ERA5

1. Introduction

The design wave is an extreme wave that is expected to be exceeded once in a long period such as 30, 50, 100, 200 years. The design wave height is calculated by the extreme wave statistics analysis. For this purpose, the long-term climate data are obtained for the study region; the annual maximum data or peak values higher than a threshold wave height are determined. Therefore, reliable and the long-term wave data are necessary for the design of various kind of coastal and harbor structures. The sources of wave data can be divided into three main categories: in-situ measurements, remotely sensed observations

* Corresponding author.
E-mail addresses: berguzarozbahceci@iyte.edu.tr (B. Oztunali Ozbahceci), ahmetturgut@iyte.edu.tr (A.R. Turgut), ahmetbozoklu@iyte.edu.tr (A. Bozoklu), saleh.abdalla@ecmwf.int (S. Abdalla).

https://doi.org/10.1016/j.asr.2020.02.021
0273-1177/

and numerical model estimates (Abdalla, 2013). Although in-situ measurements produce one of the most reliable sources of wave data, measurement data can be usually obtained for a short term due to the practical problems associated with the measurements and their expense. State Meteorological Organization in Turkey started to permanent wave measurements in Istanbul, Canakkale, Antalya and Mersin. However, the longest duration of any dataset is not more than 5 years. Some other wave measurement campaigns were also organized but unfortunately all of them lasted less than 3 years.

Satellites that are equipped with instruments capable of observing ocean waves like Radar Altimeter (RA) and Synthetic Aperture Radar (SAR) provide remotely sensed observations data. Such data source has good global coverage and is usually very reliable. Satellites are usually designed to serve for a few years (around 3–7 years) although they last twice as long on average (Abdalla and Yilmaz, 2015). This time period is not enough to construct a record suitable for climate computations. However, it is possible to extend the duration of the measured data by combining measurements from different satellites. Vinoth and Young (2011) used the 23 years consistent altimeter data to determine extreme values of wind speed and significant wave height corresponding to a 100-yr return period. Ozbahceci (2020) indicated that the combined radar altimeter data of 27 years can be used in the extreme value analysis of the Marmara Sea.

Other two sources to find the design wave characteristics along the Turkish coasts:

1- Wind and Deep-Water Wave Atlas: Atlas is one of the main products of NATO TU-WAVES Project by Ozhan and Abdalla (2002). While wind fields produced by ECMWF (The European Centre for Medium-Range Weather Forecasts) were used for climate analysis, for the extreme analysis synoptic maps corresponding to the selected extreme storms were digitized and the wind fields were produced from digitized maps. Then, 3rd generation wave models of METU3 and WAM are used to compute the wave field. For the extreme analysis, the maximum annual wind and wave data covering 20 years for Black Sea and 17 years for Mediterranean and Aegean Seas were fitted to Gumbel distribution. The results are given in a resolution of 0.3° in longitude and 0.25° in latitude.

2-Numerical model estimates: They are commonly used because of their wide temporal and spatial coverage as well as lower cost. For example, European Centre for Medium-Range Weather Forecasts (ECMWF) has been producing wind and wave parameters for the last few decades. ECMWF has also carried out several reanalyses (e.g. ERA-Interim) to extend the climate record by several decades in the past using the same model version (Dee et al., 2011). All the reanalyses cover at least the period from 1979 to the present as shown in Table 1. ECMWF with the help of several international organizations started a new reanalysis Project (the ERA-CLIM Project). In order to produce consistent reanalysis of the climate system, reaching back in time as far as possible given the available instrumental record. In this context, firstly, ECMWF has produced the uncoupled atmospheric reanalysis ERA-20C, which covers the period January 1900 to December 2010. ERA-20C assimilates only conventional observations of surface pressure and marine wind, obtained from well-established climate data collections (Poli et al., 2016). Then, as a second phase, ECMWF has completed the production of a new global 20th-century reanalysis which aims to reconstruct the past weather and climate of the Earth system including the atmosphere, ocean, land, waves and sea ice. This coupled climate reanalysis, called CERA-20C, is part of the EU-funded ERA-CLIM2 project and covers entire 20th century data (1901–2010). Both data sets are available at 3-hour time increments. Literature study shows that new century long data have started to become an attractive source for the researchers dealing with climate studies. Verification studies indicate that ERA-20C may underestimate the wave height but the data is consistent and suitable to use in climate studies (Abdalla, 2013, Abdalla and Yilmaz, 2015, Dafka et al., 2016, Patra and Bhaskaran, 2017, Dada et al., 2016, and Kumar et al., 2016). Stopa (2018) compared the wave hindcasts performed by WAVEWATCH-III model using 10 reanalysis wind field datasets including ERA-20C and 2 datasets

Table 1
Summary of reanalysis datasets of ECMWF.

Name	IFS cycle/year in operation	Atmospheric model surface spatial resolution	Ocean wave model spatial resolution	Period	Notes/references
ERA-Int	CY31R2/2006	79 km	110 km	1 Jan. 1979 to 31 Aug. 2019	Full observing system/Dee et al. (2011)
ERA-20C	CY38R1/2012	125 km	165 km	1 Jan. 1900 to 31 Dec. 2010	Conventional observations, sea surface temperature & climate data/Poli et al. (2016)
CERA-20C	CY41R2/2016	125 km	165 km	1 Jan. 1901 to 31 Dec. 2010	As in ERA-20C but with coupling to ocean circulation model/Laloyaux et al. (2017)
ERA5	CY41R2/2016	30 km	40 km	1 Jan. 1979 to 5 days behind real time (to be extended backwards to 1950)	Full observing system/Hersbach et al. (2020)

composed of merged satellite observations of the wind and concluded that ERA-20C captures overall climate variability and the magnitude of the extreme events especially in the extra tropics and it is less sensitive to changes of the data assimilated.

In the extreme value statistics performed to calculate design wave height, the cumulative probability distribution of the wave data is obtained; fitted to some theoretical distribution function and then extrapolation is performed to estimate the design wave height corresponding to the low probability of occurrence that is once in a given return period. In order to avoid the extrapolation which may cause erroneous results in the estimation of the design wave height in case of small number of wave data, 20th century wave data including 110- year time series (1901–2010) like ERA-20C and CERA-20C can be good alternatives. However, ERA-20C or any century long data have not been used to determine the extreme waves along the Turkish coasts, yet.

In this study, 110-year time series of the significant wave height and the mean wave period data of ECMWF were verified and calibrated using combined and extended satellite radar altimeter records. Although there are a number of studies showing that the satellite data are reliable (Abdalla et al., 2011), any comparison study has not been done for Turkish coasts yet. In this study, for the first time, the satellite altimeter data are verified against local in-situ data before using them for the calibration of CERA-20C data. Altimeter significant wave height data of Jason family of satellites (TOPEX, Jason-1 and 2) and Envisat family of satellites (ERS-2 and Envisat) are inter-calibrated to get the consistent satellite data sets. After the extensive calibration study, the calibrated CERA-20C wave height data were verified against local in-situ measurements. Furthermore, the mean wave period, which is not provided as part of the available altimeter observations, was estimated from the altimeter backscatter coefficients (Ku and C bands) and the significant wave height using Artificial Neural Network (ANN) Method. Estimated periods were used to calibrate the CERA-20C wave periods.

This paper is organized as follows: Section 2 provides an overview of the ECMWF, in-situ measurement and the altimeter data used in the study. The calibration study of the significant wave height is provided in Section 3. Verification analysis of the significant wave height is presented in Section 4 and the estimation of the wave period from the altimeter data by using ANN method is given in Section 5. Section 6 provides the error assessment for the verification study of both significant wave height and mean wave period. Finally, conclusions are presented in Section 7.

2. Data used

2.1. ERA-20C and CERA-20C data

Both ERA-20C and CERA-20C (see Table 1) datasets of the significant wave height were made available for the period from 1 January 1901 to 31 December 2010 with a temporal resolution of 3 h. The horizontal grid spacing is approximately 165 km for the wave model. The native model grids (default points) were retained in this study in order to avoid the problems due to numerical interpolation. In total, 40 default grid points for the wave data were selected along the Turkish coasts as indicated in Fig. 1. There are 16 grid points in the Black Sea and 24 points in Aegean Sea and the Mediterranean. Since there is no CERA-20C data, the coasts of Sea of Marmara are left out of the scope of this study.

2.1.1. Comparison of ERA-20C and CERA-20C data

In order to decide which century-based data set is appropriate to use in the study, both ERA-20C and CERA-20C were compared with Envisat Radar Altimeter (RA-2) data over the whole Black Sea for 2007–2008 as a pilot study. 16 default grid points of ERA-20C and CERA-20C in the Black Sea were determined for the comparison study. The significant wave height (Hs) data from ERA-20C and CERA-20C are compared with those of Envisat RA-2. The two datasets were assessed statistically in terms of the correlation coefficient, the bias and the standard deviation of the difference (SDD). Table 2 presents the statistical error measures of ERA-20C and CERA-20C against Envisat for the significant wave height.

Although Table 2 shows that the two datasets give similar results, CERA-20C seems to be slightly better considering the used statistical error measures. Therefore, efforts will be focussed on CERA-20C dataset only.

2.2. In-situ data

Several project-based wave measurement campaigns have been organized for a short term in Turkey. One of them was organized within the framework of NATO TU-WAVES project (Özhan and Abdalla, 1999). Five directional wave buoys were deployed at Alanya, Dalaman, Bozcaada, Sinop and Hopa (see Fig. 2 for their locations) along the Turkish coasts. Due to several practical problems like loss and damage, measurements from those wave buoys were discontinued several years ago. Measurement details can be found in Özhan and Abdalla, 1999. Location, deployment depth, distance from the coast and measurement period of each buoy are presented in Table 3.

In 2013, the State Meteorological Organization of Turkey (SMO) started to carry out permanent offshore wind and wave measurements in Silivri. Then, further measurement campaigns were organized in 2015 by SMO in Bogaz, Canakkale, Antalya and Silifke. The locations of the SMO (and NATO-TU Waves) buoys are shown in Fig. 2. A SEAWATCH Midi 185 Buoy equipped with an ultrasonic anemometer is used to collect the wind and wave data. Hourly data are provided. Locations, deployment depths, distances from the coast and measurement periods of the SMO buoys are summarized in Table 4. It should be noted that the measurement periods given in Table 4 cover several measurement gaps.

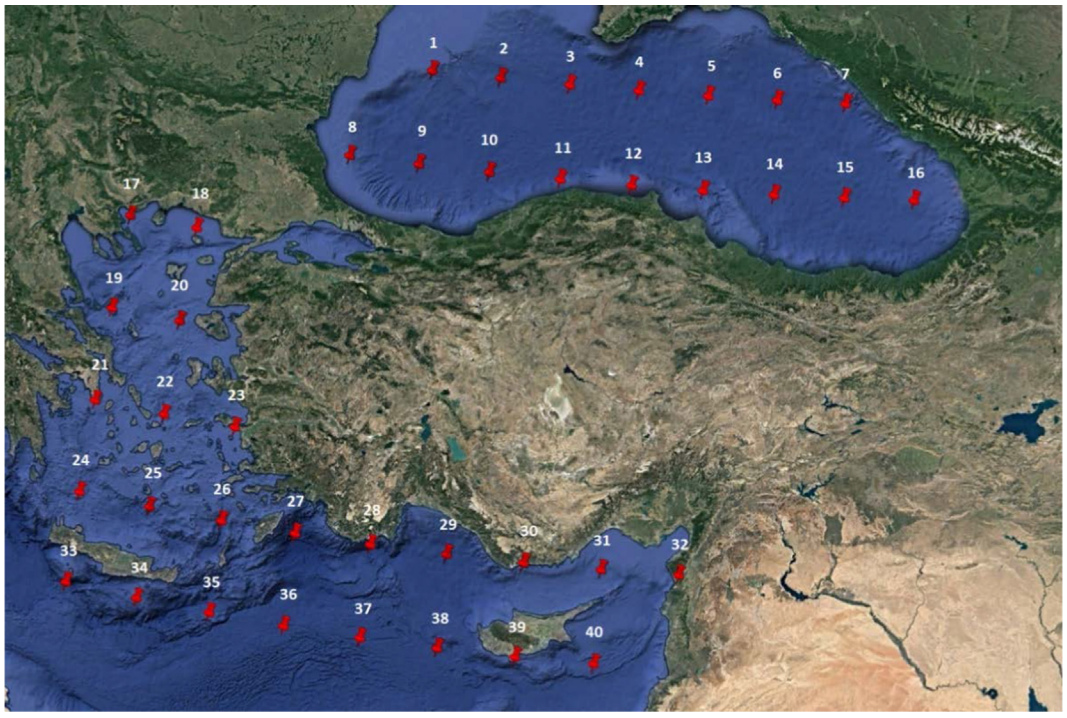

Fig. 1. Default grid points of ERA-20C and CERA-20C wave model along the Turkish coasts.

Table 2
Statistical error measures for ERA-20C and CERA-20C significant wave height against Envisat RA-2.

		ERA-20C			CERA-20C		
Latitude	Longitude	R^2	Bias (Satellite - Model)	St Dev. (Satellite - Model)	R^2	Bias (Satellite - Model)	St Dev. (Satellite - Model)
43.5	28.5	0.741	0.330	0.351	0.707	0.250	0.372
43.5	30	0.719	0.178	0.397	0.692	0.130	0.426
43.5	31.5	0.867	0.303	0.369	0.819	0.250	0.349
43.5	33	0.686	0.364	0.445	0.790	0.339	0.391
43.5	34.5	0.721	0.280	0.437	0.665	0.341	0.468
43.5	36	0.730	0.246	0.393	0.731	0.302	0.391
43.5	37.5	0.700	0.350	0.364	0.750	0.364	0.338
43.5	39	0.166	0.449	0.420	0.116	0.503	0.431
42	28.5	0.685	0.208	0.379	0.704	0.137	0.382
42	30	0.601	0.313	0.483	0.649	0.296	0.454
42	31.5	0.549	0.415	0.483	0.660	0.353	0.431
42	33	0.642	0.498	0.426	0.678	0.526	0.421
42	34.5	0.541	0.465	0.406	0.583	0.444	0.389
42	36	0.734	0.465	0.381	0.732	0.494	0.395
42	37.5	0.790	0.444	0.406	0.830	0.450	0.387
42	39	0.619	0.441	0.324	0.590	0.477	0.340
42	40.5	0.724	0.447	0.404	0.745	0.474	0.422

2.3. Verification of CERA-20C wave data against local in-situ measurements

After deciding to use the CERA-20C data in the rest of the study, the CERA-20C data were verified against available local in-situ measurements to decide whether calibration was necessary or not. Since CERA-20C does not cover any period beyond December 2010, the wave data of CERA-20C can be verified using the buoy wave measurements collected as part of the NATO TU-Waves Project between 1994 and 1999. For the purpose of the current study, the verification is performed by Quantile-Quantile plots (Q-Q plots). This choice was made to maintain the agreement between the CERA-20C and the buoy data in terms of probability distributions which is more important than the one-to-one agreement for the extreme value analysis. In order to calculate the quantiles, CERA-20C default grid point closest to the measurement location is determined. All the data of the CERA-20C and the buoy collected in the same time period (daily) are used without considering whether they are collocated in exact time or not. Then the quantiles corresponding to same non-

Fig. 2. Locations of measurement buoys (yellow: SMO, pink: NATO-TU waves) around Turkey. (For interpretation of the references to colour in this figure legend, the reader is referred to the web version of this article.)

Table 3
Location, deployment depth, distance from the coast and measurement period of each NATA-TU-Waves Project buoy.

Station	Latitude	Longitude	Water depth (m.)	Distance from coast (km)	Measurement Period (YMD)
Alanya	36° 32′ 30″ N	31° 58′ 30″ E	100	1.4	19941101–19960208
Dalaman	36° 41′ 30″ N	28° 45′ 18″ E	100	1.0	19941121–19960729
Bozcaada	39° 42′ 14″ N	26° 02′ 57″ E	62	13.2	19941128–19950926
Sinop	42° 07′ 24″ N	35° 05′ 12″ E	100	11.6	19941201–19960614
Hopa	41° 25′ 24″ N	41° 23′ 00″ E	100	4.6	19941227–19990426

Table 4
Locations, deployment depths, distances from the coast and measurement periods of the buoys of SMO.

Station	Latitude	Longitude	Water depth (m.)	Distance from coast (km.)	Measurement period (years)
Silivri	40.9742	28.2487	50	4	2013–2018
Bogaz	41.2922	29.1656	75	8	2015–2018
Canakkale	40.0483	26.0356	70	11	2015–2018
Antalya	36.7167	31.0167	330	13	2015–2018
Silifke	36.0800	33.8300	180	14	2015–2018

exceedance probabilities are calculated. As a result, Q-Q plots are graphed by plotting their quantiles against each other. Q-Q plots of buoy significant wave height measurements at Hopa, Sinop, Bozcaada, Dalaman and Antalya are plotted against their counterparts from the CERA-20C data together with the line y = x and are shown in Fig. 3.

Fig. 3 shows that CERA-20C wave model underestimates wave heights at Hopa, Sinop, Dalaman and Alanya and overestimates them at Bozcaada. It was reported that the 20th century reanalysis in general underestimates significant wave height (see for example Stopa, 2018, and Abdalla and Yilmaz, 2015). This was indeed the case for the buoys located in the Black Sea (Hopa and Sinop) and the Mediterranean (Alanya). However, for the buoys in Aegean Sea (Bozcaada and some extend Dalaman) which contains many unresolvable islands, CERA-20C overestimates wave heights. Note that CERA-20C underestimates high waves at Dalaman buoy due to existence of a narrow window with a long fetch.

Q-Q plots of mean wave period, Tm, between CERA-20C and in-situ measurements around the coasts of Turkey are shown in Fig. 4. The mean wave period is defined as a mean over all frequencies and directions of the two-dimensional wave spectrum. It is clear that CERA-20C provides mean wave period estimates better than the significant wave height. In particular, CERA-20C underestimates wave periods compared to the buoy measurements at Hopa (in the Black Sea) for most of the points. However, at Sinop (the other buoy in the Black Sea) CERA-20C gives very close wave periods to the measurements except for the high wave periods where a slight underestimate can be seen. In the Aegean Sea, CERA-20C overestimates the wave period compared to the buoy measurements at Bozcaada due to the missing of the unresolvable islands in the model. However, at Dalaman

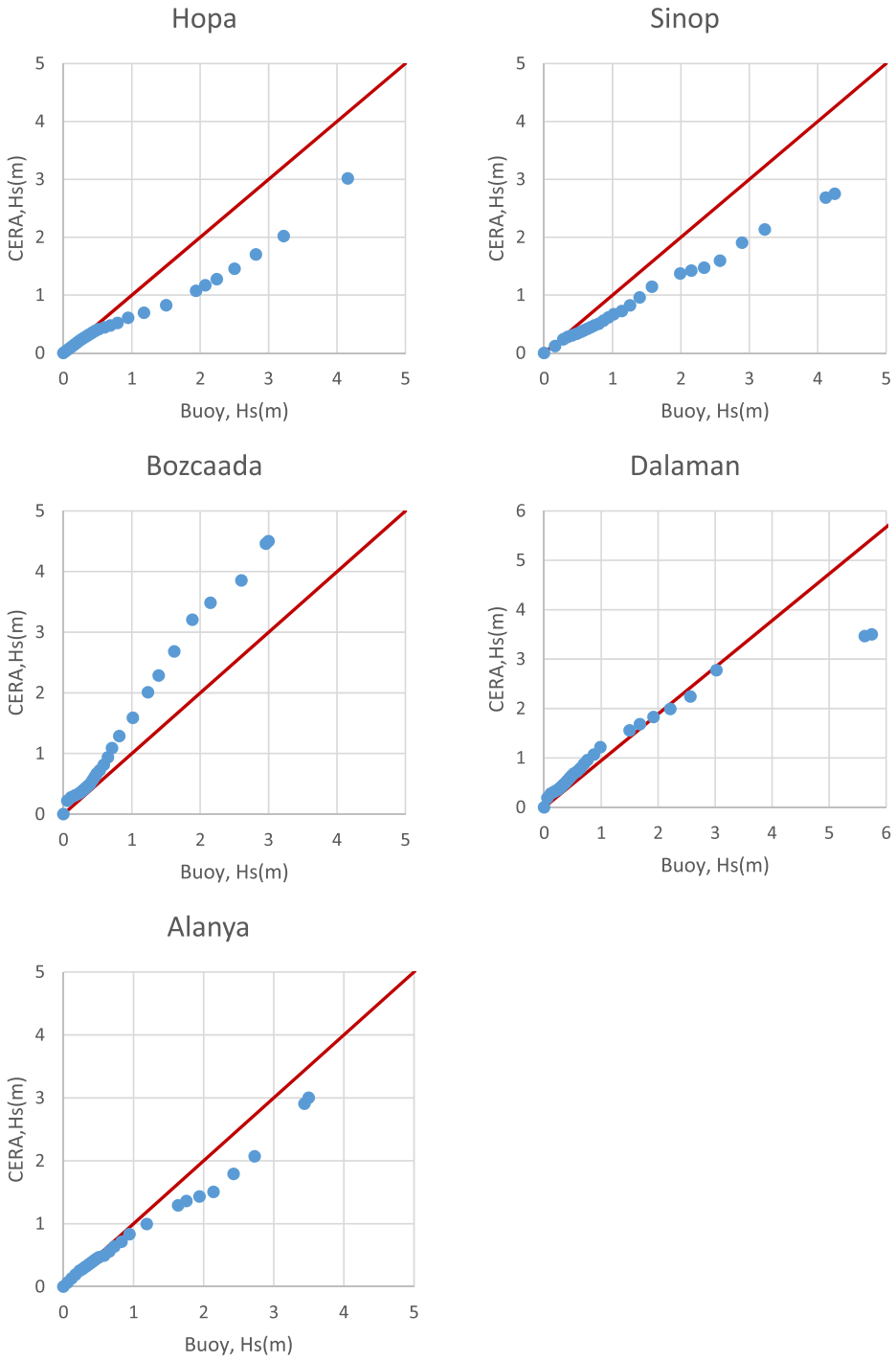

Fig. 3. Q-Q plots for CERA-20C Hs versus buoy measurements at the five TU-WAVES buoys. Diagonal continuous lines represent the symmetric y = x line.

the wave period agreement is quite good with a tendency of CERA-20C to overestimate wave periods below 6 s and overestimate higher wave periods. At Alanya in the Mediterranean, CERA-20C gives comparable wave periods to those of the buoy below 6 s and slightly higher wave periods above that value.

Figs. 3 and 4 show that CERA-20C significant wave height data and the wave period data, especially in the Aegean Sea, need to be calibrated before they can be used for the extreme wave analysis along the Turkish coasts.

2.4. Satellite radar altimeter data

Buoy wave data of SMO mentioned in Table 4 cannot be used for the calibration of CERA-20C dataset, which covers the period until 2010, because SMO measurements were started in 2013 and 2015. Furthermore, the data of

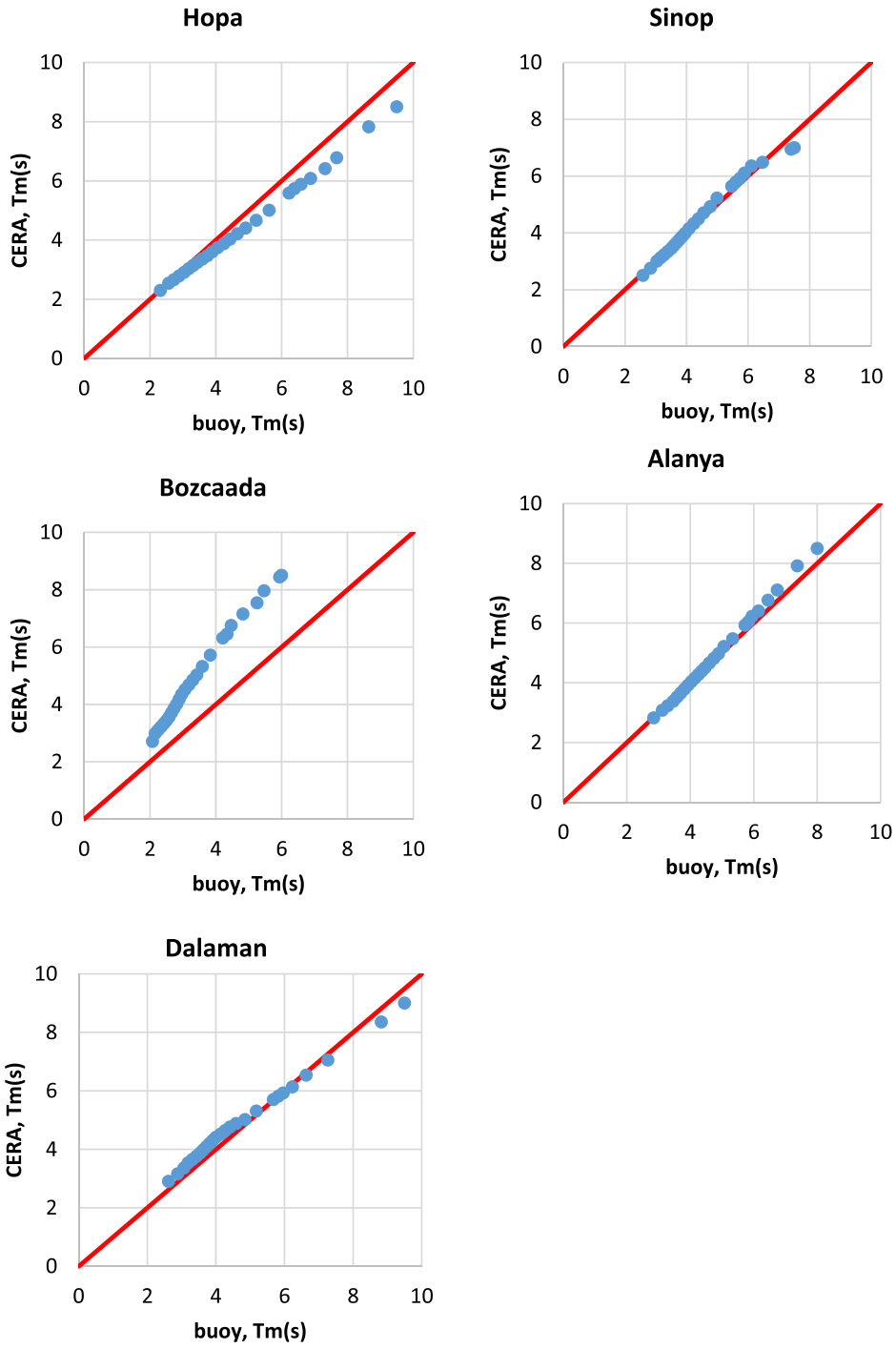

Fig. 4. Q-Q plots for CERA-20C Tm versus buoy measurements at the five TU-WAVES buoys. Diagonal continuous lines represent the symmetric y = x line.

NATO-TU-WAVES buoys measured between 1994 and 1999 are reserved as the "ground truth" for verification purposes. Therefore, it was decided to use the satellite data for the calibration of CERA-20C data.

Satellites that are equipped with Radar Altimeter (RA) instruments are capable of observing ocean significant wave height (see for example Abdalla and Janssen, 2018). Janssen et al. 2007 and Abdalla et al. (2011) showed using a triple collocation technique that at the scale of the model (around 75 km) the random error of altimeter Hs is almost 6% of mean Hs. This is a global error value that is valid at the locations of the buoys reporting data through the Global Telecommunication System (GTS) of World Meteorological Organisation (WMO). Those buoys are mainly located around Europe and North America. Even it was shown that the altimeter dataset have a good global coverage and are usually very reliable (Janssen et al., 2007, Abdalla et al., 2011; Abdalla and Janssen, 2018). The first

step is to verify the altimeter data against the in-situ observations. The second step is to use them for the calibration of CERA-20C data.

To verify the radar altimeter against the in-situ measurement data, ideally, it is desirable to collocate the altimeter and buoy observations at no spatial or temporal difference (Abdalla et al., 2011). However, such restriction severely limits the number of collocations. Therefore, a trade-off between tolerating differences in time and space from one side and obtaining enough collocations to produce meaningful statistics from the other side. As a result, the matchup areas shown in Fig. 5 were selected for SMO buoys in Bogaz, Silivri, Canakkale, Antalya and Silifke such that buoy and satellite data separated by no more than 0.5 deg in latitude/longitude (about 40–45 km) as recommended by Young et al. 2011. The size of the match-up areas was also restricted by the surrounding orography to avoid match-ups behind islands and peninsulas. The matchup time was determined as 30 min considering the hourly buoy measurement. Young et al. 2011 recommend the matchup time as no more than 30 min. RA data of satellites recorded in the defined matchup areas was retrieved from the RADS (Radar Altimeter Database System) developed first at Delft University of Technology (Scharroo et al., 2013). Jason-2, SARAL/AltiKa, CryoSat-2, Jason-3 and Sentinel-3A are the satellite missions with the available significant wave height data during the measurement periods of in-situ data given in Table 4. In order to increase the collocation number, all the altimeter data (Jason-2, CryoSat-2, SARAL/AltiKa, Jason-3 and Sentinel-3A) were combined and one satellite database was obtained for each buoy location. Before the collocation step, RA data was filtered to remove inconsistencies and outliers. For filtering, Ku band and C band backscatter coefficients, standard deviation of Ku band range and standard deviation of Ku band significant wave height values were used. The data with the standard deviation of Ku band range > 0.15 m and the standard deviation of Ku band significant wave height > 1 m were removed firstly. Then the data along the satellite track in the matchup area and the time are checked. The data with the significant wave height difference $\Delta Hs > 1$ m for the same record time are also removed to avoid outlier data. ΔHs is defined as the absolute value of the difference $Hs\text{-}Hs_{avg}$, where Hs_{avg} is the average of the selected sequence of measurements. Q-Q plots for Hs of the altimeter measurements versus SMO buoy measurements are presented in Fig. 6.

Q-Q plots for Hs given in Fig. 6 indicate that the altimeter measurements agree well, in terms of Q-Q, with the buoy measurements especially in Bogaz and Çanakkale. However, the altimeters give higher significant wave height values in the other three locations. The reason may be the effect of unavoidable 'land contamination' close to the coastal area on the quality of the satellite data and may also be due to spatial differences between the RA and the buoy measurements.

Based on the time series comparisons, statistical error measures of RMSE (root mean square error), SI (scatter Index = RMSE/mean value of the Hs of the buoy), bias, symmetric slope, A defined as $y = A\,x$, and the correlation coefficient, R, are calculated and the results are presented together with the data numbers and the mean values of

Fig. 5. Locations of the SMO measurement stations and the used matchup areas.

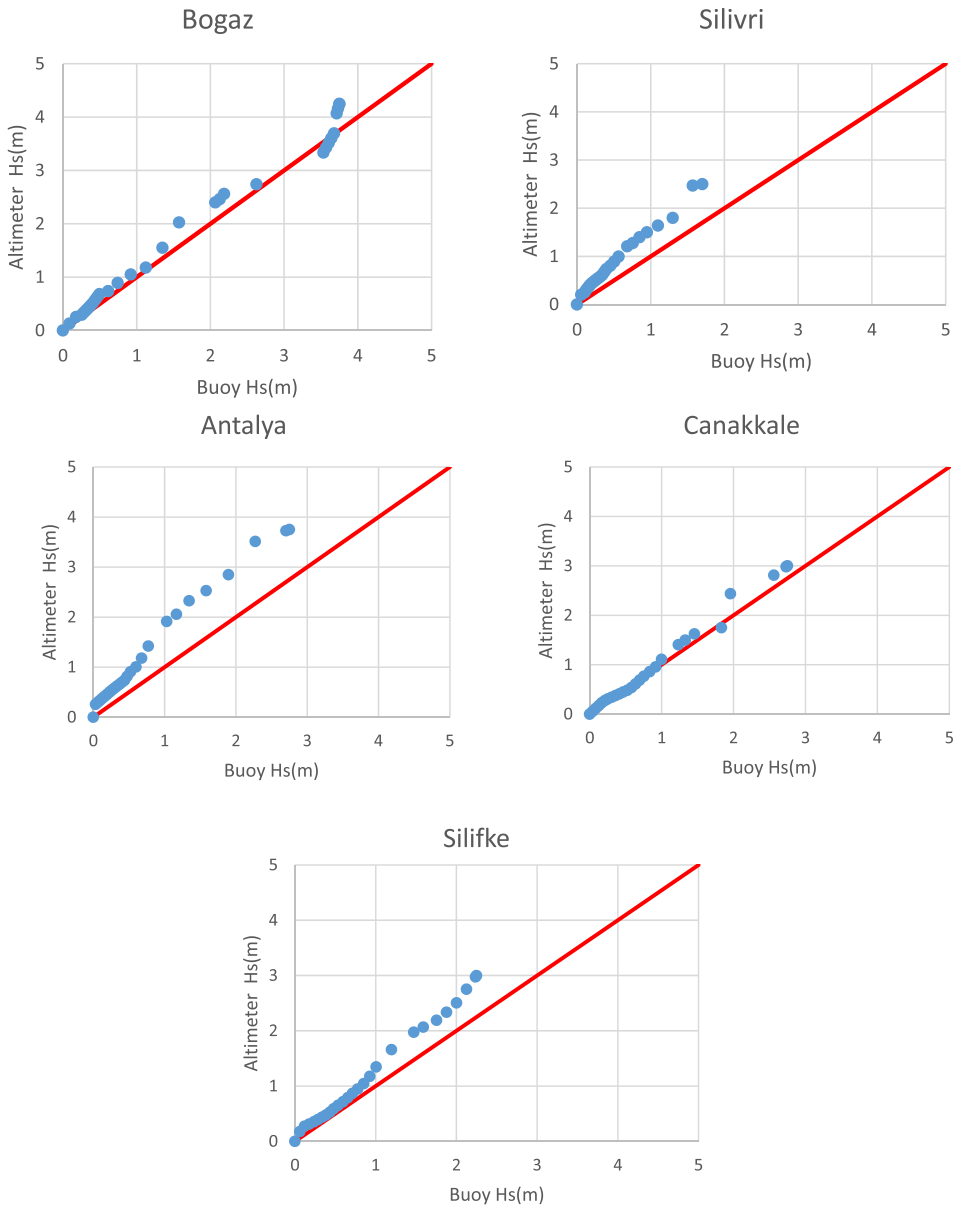

Fig. 6. Q-Q plots for Hs of the SMO buoy measurements versus altimeter measurements.

altimeter and buoy significant wave heights in Table 5. The term "error" hereafter should be interpreted as the difference between the two datasets rather than a proper measure of the error.

Table 5 shows that the error is high when the altimeter records of Hs are compared against their SMO in-situ counterparts. One possible explanation for the high is the limited amount of the used data (see Table 5) due to both limited altimeter data in the matchup areas and the limited duration of the wave measurement (see Table 4). Furthermore, the offset between the actual position of the buoys (closer to the coast) and the matchup areas (slightly offshore) contributes to the differences. At the Antalya measuring station, for example, the offset between the actual

Table 5
Error assessment for the significant wave height, Hs, of the combined satellite RA data against the SMO buoy measurements.

Buoy location	data no	RMSE	SI	bias	A	R	RA (mean)	Buoy (mean)
Bogaz	72	0.2378	0.2799	0.1482	1.1098	0.9817	0.9977	0.8496
Silivri	603	0.3799	1.2134	0.2724	1.5510	0.5763	0.5855	0.3131
Canakkale	147	0.3230	0.5821	0.0065	0.9319	0.7229	0.5613	0.5548
Antalya	383	0.4823	1.1677	0.3433	1.6086	0.8031	0.7564	0.4131
Silifke	176	0.3029	0.4419	0.1273	1.1929	0.8830	0.8127	0.6855

location of the buoy and its match-up area is the largest among the SMO stations (Fig. 5). The deviations between the altimeters and the buoy measurements at Antalya (Fig. 6) are the highest.

Although the two Hs datasets show deviations when it comes to the time series comparisons, their probability distributions, as emerging from the Q-Q plots, show more similarities. Considering the results of the comparison between the satellite RA data and the SMO buoy data, it was clear that another approach is needed.

ECMWF recently released the latest model reanalysis dataset called ERA5 which was produced as part of the European Commission Copernicus Climate Change Service (C3S). ERA5 provides hourly estimates of a large number of atmospheric, land and oceanic climate variables. The atmospheric data cover the Earth on a 30-km grid

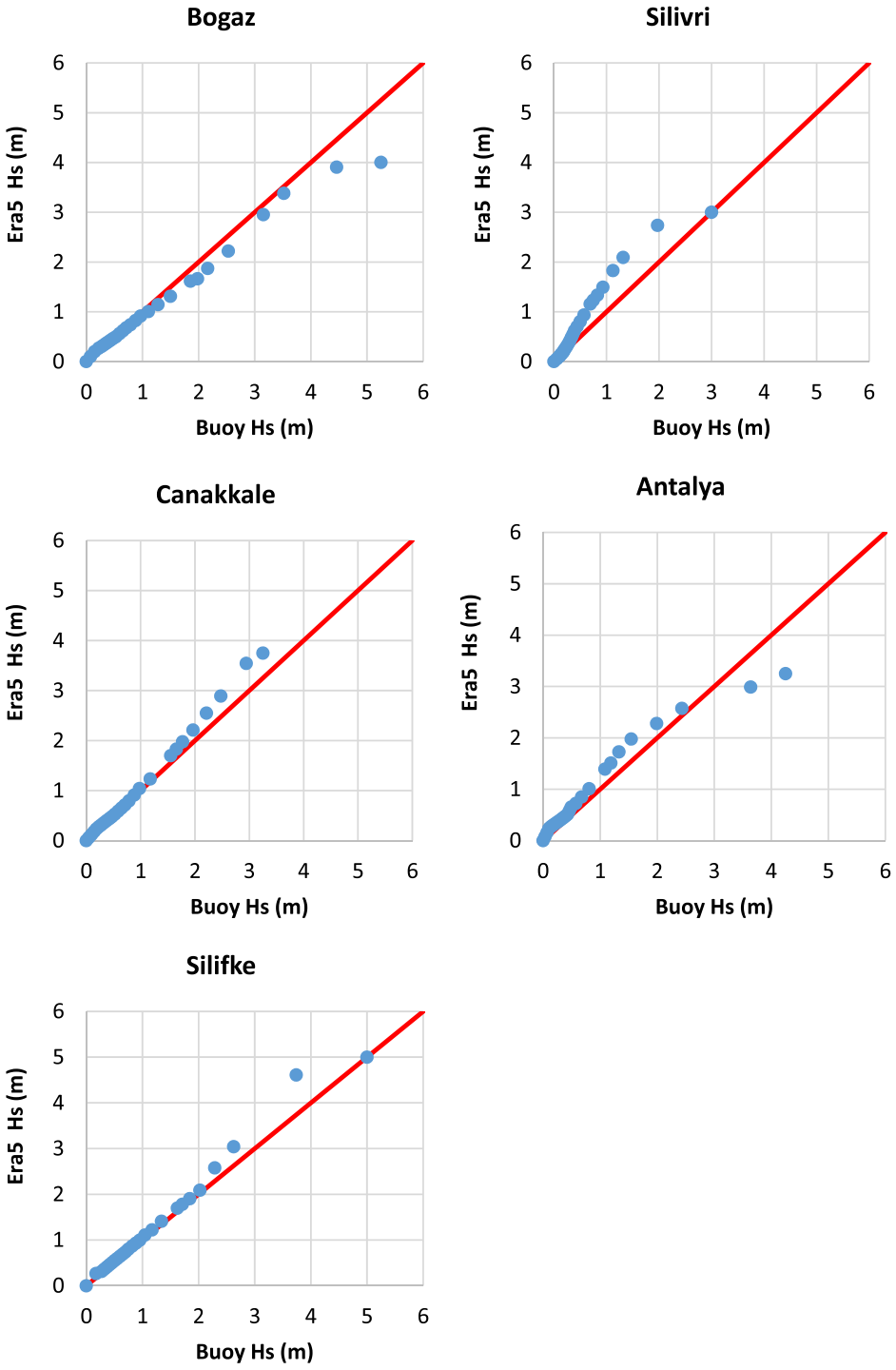

Fig. 7. Q-Q plots of ERA5 Hs data versus the buoy Hs data at the five measuring stations of SMO.

Table 6
Error assessment for Hs of ERA5 data against the buoy measurements.

Buoy location	Data No	RMSE	SI	Bias	A	R	ERA5 mean	Buoy mean
Bogaz	10,460	0.2165	0.2903	−0.054	0.8844	0.93860	0.6925	0.746
Silivri	36,811	0.3231	1.0466	0.1304	1.3029	0.62420	0.4391	0.3087
Çanakkale	8237	0.2578	0.4398	0.0346	1.0188	0.86420	0.6209	0.5863
Antalya	13,520	0.2495	0.5962	0.1227	1.1512	0.84920	0.5412	0.4185
Silifke	14,481	0.2762	0.3704	0.0497	1.0187	0.83460	0.7953	0.7456

while the ocean waves are available on a 40-km grid (see Table 1 and Hersbach et al., 2020). ERA5 dataset is now available for public use (from 1979 to within 5 days of real time with a planned backward extension till 1950 soon). ERA5 represents the best available open dataset for climate computations in terms of consistency and resolution. Therefore, it was decided to use it as a second reference after verification and calibration.

Q-Q plots for Hs of ERA5 analyses versus SMO buoy measurements are presented in Fig. 7. The deviations between the probability distributions of ERA5 and the SMO buoy datasets in terms of Q-Q comparison is relatively small at the buoys in rather open water (all except Silivri). Silivri buoy is located in the Sea of Marmara which is a small water body. The 40-km ERA5 grid is too coarse to represent the basin (mainly ERA5 model increases the fetch lengths in Sea of Marmara and thus the higher wave height estimates at Silivri buoy).

The error statistics based on the time series comparison were also calculated and the results are presented in Table 6. Compared to the statistics presented in Table 5 for Altimeter-buoy comparison, Table 6 (ERA5-buoy) show less differences. The differences at Silivri buoy is still rather high for the same ERA5 resolution reason mentioned above. The amount of the data collocations (tens of thousands for ERA5 compared to few hundreds for the altimeter verifications) plays an important role in reducing the differences as well.

Both Fig. 7 and Table 6 show that the difference between ERA5 and in-situ datasets is much less compared to difference between the satellite and the buoy sets. Therefore, it was decided to use ERA5 data as a second reference in addition to the satellite data for the calibration of CERA-20C significant wave height.

3. Calibration of CERA-20C data

The duration of data that can be obtained from any of the satellites usually does not exceed 15 years due to the lifetime of the satellites (Ozbahceci, 2020). Combining measurement data from more than one satellite can extend the duration of the continuous altimeter time record to more than two decades. However, the characteristics of the measurements of various altimeters are different. Therefore, any attempt to carry out climate computations from combined radar altimeters must involve an inter-calibration exercise (Abdalla, 2013, Young and Sanina, 2017).

In order to be able to calibrate CERA-20C data, radar altimeters with available data before 2010 are checked. It is noticed that the Jason family of satellites (TOPEX/Poseidon, Jason-1 and 2) which has a 10-day repeat cycle and ENVISAT family of satellites (ERS-1, ERS-2 and ENVISAT) with a repeat cycle of 35 days have the data before 2010 in the study area. The measurement and the overlap periods of these family satellites are given in Fig. 8. As it can be seen in Fig. 8, measurement period of one satellite mission overlaps the next. In this study collocated records in overlap periods are used for inter-calibration of the satellites.

For the inter-calibration of the satellites using the overlap periods, first of all, the satellite data were retrieved from RADS website by defining the matchup area for each of the 40 default grid points of CERA-20C given in Fig. 1.

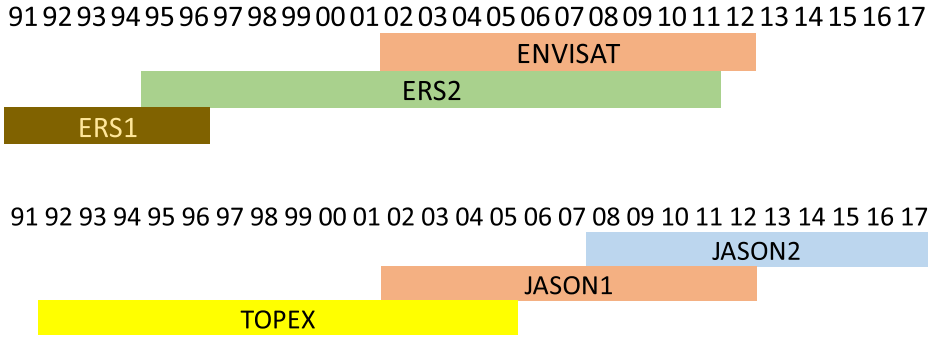

Fig. 8. The measurement and the overlap periods of ENVISAT and JASON family satellites. Note that the degraded coverage of ERS-2 after 2003 does not impact the availability of ERS-2 data in the study area.

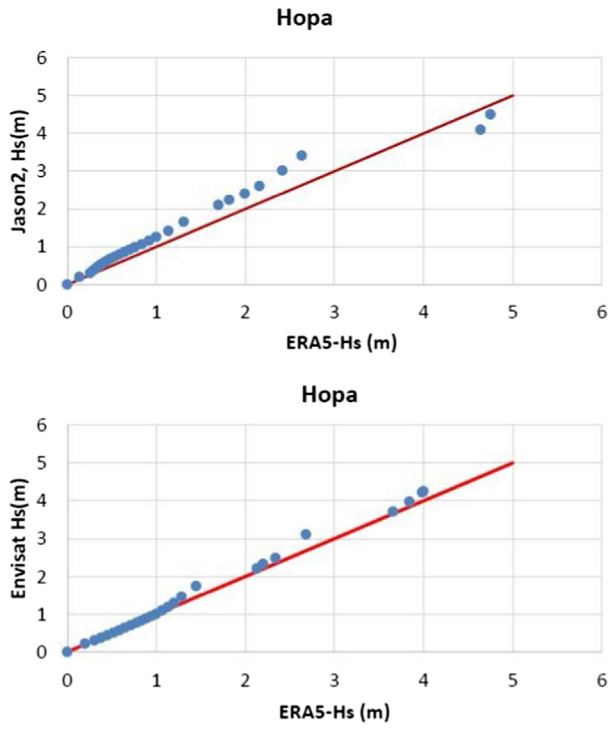

Fig. 9. Q-Q plots for Hs of ERA5 versus Envisat and Jason-2.

Calibration of the altimeter significant wave height at the 16th grid point shown in Fig. 1, in the Eastern Black Sea near Hopa is given as an example. After all the satellite data were retrieved and filtered as explained in Section 2.4, Hs of Jason-2 data from Jason satellite family and Hs of ENVISAT data from ENVISAT satellite family were compared with ERA5 Hs data to decide which families of satellites were appropriate to use in the calibration of CERA-20C for that grid point, especially considering the largest sea states. Q-Q plots of the comparison are demonstrated in Fig. 9. Even if ERA-5 may be considered as "contaminated" by altimeter data, the impact on CERA-20C would not be that significant since Q-Q calibration was used and the assimilation impact on the bias is negligible by design.

Fig. 9 shows that ENVISAT Hs has better agreement with the Hs of ERA5. Therefore, ENVISAT satellite family (Envisat, ERS2, ERS1) was selected for the calibration of CERA-20C data for the 16th grid point.

Then, Hs data of ERS-2 was inter-calibrated with respect to Hs data of ENVISAT using overlapping measurement period shown in Fig. 8. Inter-calibration means that the comparison of the overlapped data of two different satellites. If the agreement is not good, previous data set is calibrated with respect to the recent dataset. For the calibration, linear regression was used assuming a linear relationship between the two data sets. Fig. 10 shows an example Q-Q plot between ERS-2 and ENVISAT. The good agreement of the two distributions can be inferred from falling all Q-Q pairs on the symmetric line. Since the agreement was found to be good, ERS-2 and ENVISAT altimeter datasets were combined without any calibration.

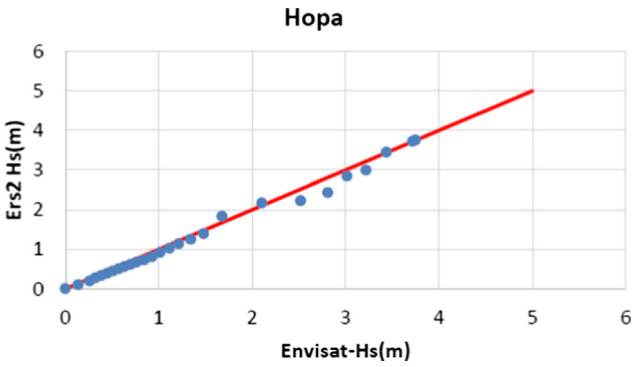

Fig. 10. Q-Q plot for the comparison of ERS-2 and ENVISAT in terms of Hs for the overlapping period (2002–2011).

Although there is an overlap period between ERS-2 and ERS-1 (1995 and 1996) as indicated in Fig. 8, it could not be possible to find any ERS-1 measurements in the match-up areas for the same period of ERS-2 thus hindering the possibility to carry out any inter-calibration between the two satellites. Therefore, it was only possible to combine ENVISAT and ERS-2 data for the ENVISAT satellite family and to obtain a combined inter-calibrated dataset of Hs with a total duration of 18 years (1995–2012). Then, combined inter-calibrated ERS-2 and ENVISAT altimeter data were used to calibrate CERA-20C.

The procedure for the calibration of CERA-20C significant wave height data is as follows. CERA-20C Hs data were compared against the combined altimeter Hs data in terms of Q-Q plot (the distributions) as shown in top panel

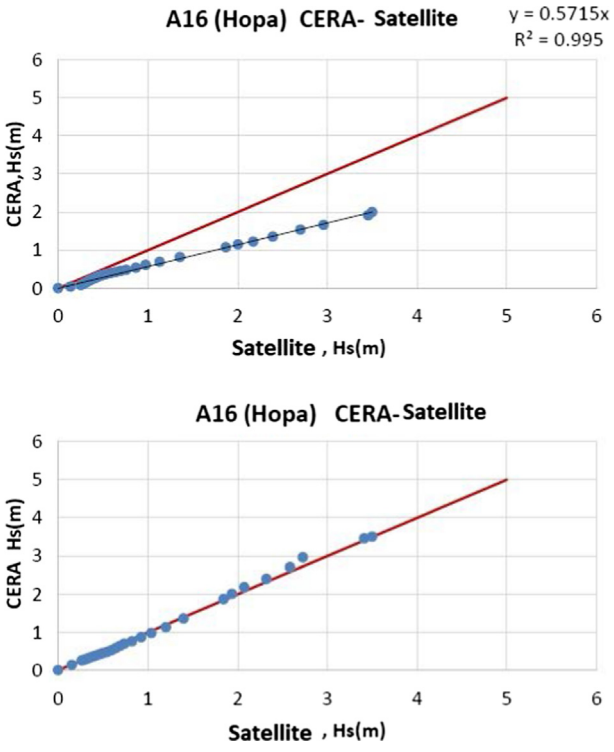

Fig. 11. Q-Q plots for Hs of CERA-20C versus Satellite RA before (upper panel) and after calibration (lower panel).

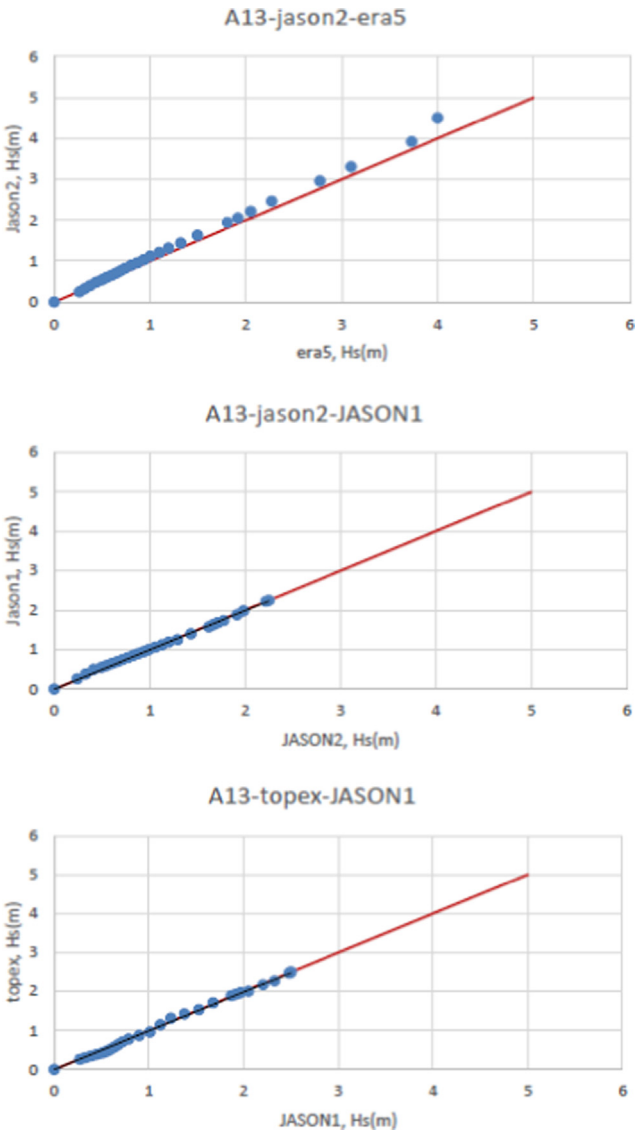

Fig. 12. Q-Q plots for the comparison of Jason-2 with ERA5 and for the inter-calibration of Jason-1 and Topex data with respect to Jason-2 in terms of Hs.

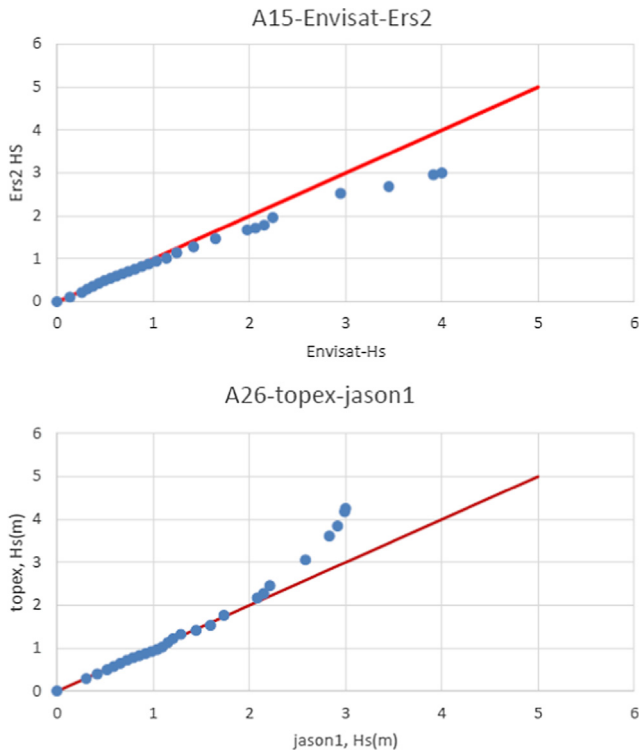

Fig. 13. Q-Q plots for the examples that the agreement between the Hs data of two satellites is not good in the overlapped period.

of Fig. 11. It is clear from Fig. 11 that CERA-20C Hs is lower than the ERS2-ENVISAT combined Hs. Assuming a linear relationship between CERA-20C and the combined altimeter dataset, the calibration was performed using linear regression to minimize the differences between CERA-20C and altimeter Hs values. This procedure ensures that the extreme sea states are well captured leading to a successful extreme wave analysis. For the same example (the 16th grid point in Fig. 1), the regression relation is $y = 0.5715\ x$ with the square of correlation coefficient, $R^2 = 0.995$ as can be seen in Fig. 11. The lower panel of Fig. 11 shows the good agreement between CERA-20C and the satellite wave height data after CERA-20C calibration.

Jason family of satellites (Jason-2, Jason-1, TOPEX) gives a better agreement with ERA5 data at several grid points. The case of A13 (13th grid in Fig. 1) is given as an example in Fig. 12. Then inter-calibration of Jason-1 and TOPEX data was performed. Results are shown in Fig. 12. After inter-calibration, Jason family satellite data were combined so that the duration of the satellite data was extended to 26 years (1992–2017).

During the inter-calibration procedure, it was observed that the agreement between two satellites data in the overlap period was good as given in Figs. 10 and 12. However, in some cases, the agreement was not good as shown in Fig. 13 for the points A15 and A26. In those cases, they were inter-calibrated with respect to the satellite data in recent years before the data were combined.

4. Verification of CERA-20C significant wave height data

After the extensive calibration, the CERA-20C significant wave height data were compared against the in-situ data measured within the framework of NATO-TU Waves Project at Hopa, Sinop, Bozcaada, Dalaman and Alanya (see Fig. 2) for the verification purposes. Fig. 14 shows the comparison between the calibrated CERA-20C Hs data against buoy measurements. It is clear that the calibrated CERA-20C significant wave heights fit well to the buoy measurement data. Considering the pre-calibration comparisons given in Fig. 3, the effect of calibration is quite remarkable especially for higher waves. Therefore, it can be concluded that the calibrated CERA-20C significant wave height data is appropriate to determine the extreme

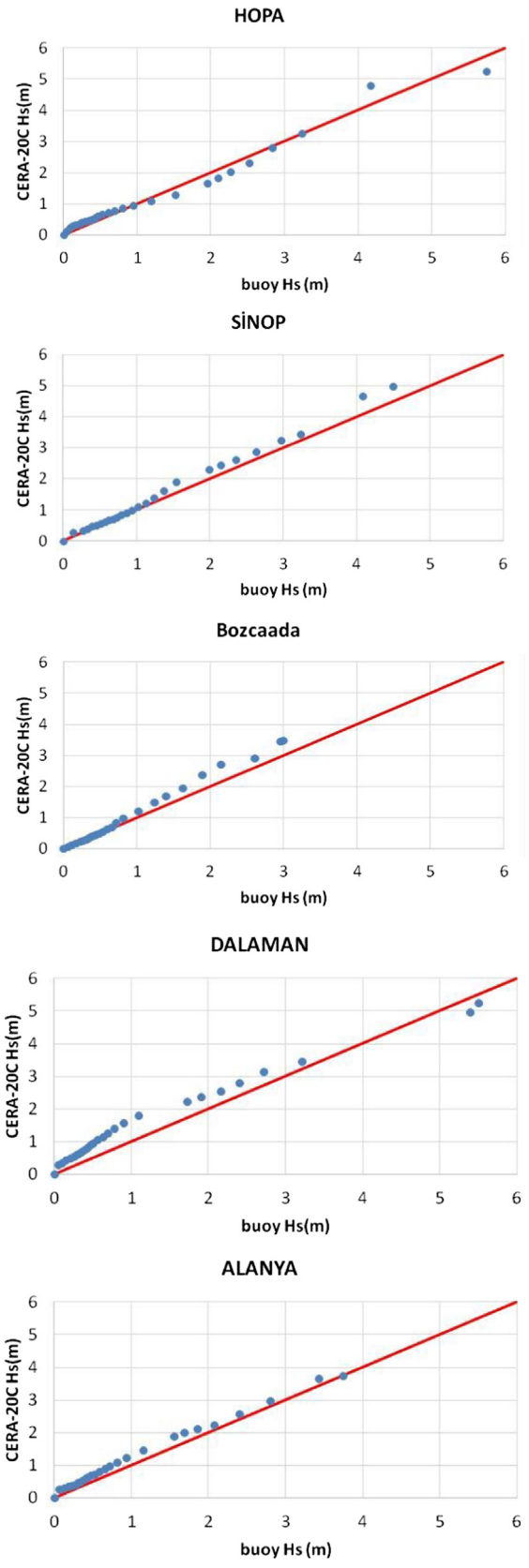

Fig. 14. Q-Q plots for CERA-20C Hs versus buoy measurements at the five TU-WAVES buoys after calibration.

waves to be used in the design of coastal structures along the Turkish coasts.

5. Estimation of the mean wave period from satellite records

Satellite radar altimeter (RA) instruments have been providing significant wave height (Hs) for all the missions and the wind speed (u_{10}). However, the wave period has never been part of the RA standard products so far. There are several methods to derive the wave period from the satellite data. Gommenginger et al. (2003) proposed a simple empirical formula with a significant wave height and back-scatter coefficient to find the wave period. Quilfen et al. (2004) used the artificial neural network method to derive mean wave period from altimeter data. Mackay et al. (2008) derived a new empirical formula for the backscatter coefficients in excess of 0.13. Badulin (2014), on the other hand, developed a physical model using wave height and positional derivative without using the backscatter coefficient to calculate the wave period.

In this study, Artificial Neural Networks (ANN) method was used to estimate the mean wave period, Tm, from the satellite data. The mean period here is defined as the reciprocal frequency moment of the full spectrum (T_{01}). Quilfen et al., 2004 compared their mean wave periods derived by ANN model with in situ measurements and concluded that high correlations gave confidence in the derived altimeter wave period parameter. In order to develop the ANN model, Jason-3 RA measurements of the significant wave height and backscatter coefficients of Ku band and C band (σKu and σC), formally known as the normalized radar cross-section (NRCS) (Quilfen et al., 2004), were used for the year 2017 as input. Calibration of estimated altimeter wave period from ANN requires reference measurements of the mean wave period provided by buoys (Quilfen et al., 2004). Since there are a few buoy measurements along the Turkish coasts (Table 4) and the buoy data was reserved for the verification of CERA-20C data, in this study ECMWF operational model data collocated with the radar altimeter data for the year 2017 were used as output.

The feed forward back propagation network model was used to predict the mean wave period, which is the most common method in modelling and estimating time series (Tayfur, 2012). Levenberg-Marquardt (LM) algorithm was used in the training of the network. The ANN model was designed as 3 inputs (altimeter Ku-band significant wave height, NRSC for Ku and C bands), 10 hidden layer neurons and 1 output (reference mean wave period from ECMWF operational model). Single hidden layer was used in the study because it is the popular method in feed-forward ANNs (Tayfur, 2012). The Tan-sigmoid transfer function is used for the training of the network.

Firstly, the neural network model was designed and trained using the global data of Jason-3 and the

Table 7
Error assessment for the mean wave period of altimeter estimated by ANN model against the reference (ECMWF operational model data).

Test cases and data number	mean of ECMWF	mean of ANN	MAE	MARE	RMSE	bias	SI	R	Slope, A
Trained by the global data (900000 data)									
Mediterranean (7613)	4.8140	5.7753	1.0080	0.2245	1.1871	0.9613	0.2466	0.8853	1.1869
Turkish coasts (3541)	4.7517	5.6482	0.9804	0.2189	1.1608	0.8965	0.2443	0.8485	1.1741
Black Sea (1234)	4.4454	5.4359	1.0247	0.2452	1.2019	0.9905	0.2704	0.8592	1.2100
Trained by the Mediterrenean Sea data (5329 data)									
Mediterranean (2284)	4.8140	4.8036	0.3755	0.0847	0.4965	−0.0104	0.1031	0.9252	0.9880
Turkish coasts (1587)	4.7517	4.6757	0.4178	0.0900	0.5827	−0.0760	0.1226	0.8834	0.9703
Black Sea (1234)	4.4454	4.5503	0.3701	0.0908	0.4797	0.1048	0.1079	0.9104	1.0129
Trained by the Turkish coasts data (2479 data)									
Mediterranean (5659)	4.4454	4.6352	0.3994	0.0991	0.5077	0.1898	0.1142	0.9097	1.0057
Turkish coasts (1062)	4.8140	4.8922	0.3892	0.0894	0.5058	0.0782	0.1051	0.9243	0.9877
Black Sea (709)	4.7517	4.7556	0.4201	0.0921	0.5745	0.0039	0.1209	0.8847	1.0315
Trained by the Black Sea data (864 data)									
Mediterranean (7613)	4.8140	4.6847	0.3950	0.0858	0.5302	−0.1293	0.1101	0.9198	0.9631
Turkish coasts (3016)	4.7517	4.5609	0.4372	0.0915	0.6161	−0.1908	0.1297	0.8803	0.9464
Black Sea (370)	4.4454	4.4411	0.3492	0.0839	0.4627	−0.0043	0.1041	0.9124	0.9890

corresponding reference wave period from ECMWF operational model. Percentages of data used for the training and testing were 70%, 30%, respectively. After the training was completed, the mean wave period was predicted not only globally but also for three enclosed sea areas: the whole Mediterranean Sea, around the Turkish Coasts (only the sea area between 25.0 and 42.0 E, 34.0–42.0 N) and the whole Black Sea. Statistical error measures of RMSE (root mean square error), SI (scatter Index), bias, symmetric slope, A (defined as $y = Ax$) and the correlation coefficient, R, are calculated and the results are presented together with the mean values of the reference mean wave period (ECMWF operational model) and the altimeter period estimated by ANN model in Table 7. As can be seen in Table 7, when the model was trained with the global data, the accuracy of the predicted mean wave period in the enclosed seas is not very high.

Three more ANN models were developed by using the Mediterranean Sea, the Turkish Coasts and the Black Sea data for the training. For each model, wave period is predicted for the three areas of the whole Mediterranean Sea, around the Turkish Coasts (only the sea area between 25.0 and 42.0 E, 34.0–42.0 N) and the whole Black Sea. Error assessment results are also given in Table 7 for the three models.

Table 7 indicates that when the model was trained with the data from the enclosed seas, the wave period predictions were significantly better than the predictions trained by the global data. High correlations and lower errors in Table 7 gave a confidence that mean wave period can be estimated from altimeter parameters for the enclosed seas using ANN model if the model is trained with the enclosed sea data.

Then the mean wave periods were predicted by the developed ANN model to compare with the buoy measurements. Fig. 15 shows the Q-Q plots for the mean period of ANN Dafka et al., 2016 model and the buoy at all the available stations of Hopa and Sinop (Black Sea), Silivri (Sea of Marmara), Canakkale (Aegean Sea), Dalaman and Alanya (Mediterranean).

Fig. 15 shows that predicted altimeter mean wave periods computed by the ANN model agree very well with their corresponding buoy counterparts. Nevertheless, the ANN model seems to overestimate the lower mean wave periods compared to the in-situ measurements.

5.1. Calibration and verification of CERA-20C mean wave period data

Original CERA-20C mean wave periods show better agreement with the buoy measurements (Fig. 4) compared to that of CERA-20C significant wave height data (Fig. 3). However, the agreement was not perfect especially at the buoy located at Bozcaada. Therefore, it was decided to calibrate CERA-20C period for Bozcaada with respect to the ANN estimates of the wave period from the altimeter data.

ANN was trained using the regional satellite (Jason-2) data covering the period from 2008 to 2016 to produce the mean wave period from the altimeter measurements, hereafter will be called altimeter mean wave period. Next, the altimeter mean wave period dataset is used to calibrate CERA-20C wave period data. Fig. 16 shows the Q-Q plot of the altimeter (ANN) and CERA-20C mean wave periods. The relation between altimeter (ANN) and CERA-20C wave periods in Fig. 16 is clearly not linear. Therefore, a quadratic regression function was used to fit this relation in Fig. 16. This quadratic function was used to calibrate CERA-20C Tm data. The calibrated wave period data were then compared against their buoy counterparts for verification purposes. Fig. 17 shows the Q-Q plots of CERA-20C Tm versus those of the buoy at Bozcaada before and after the calibration. As can be seen from Fig. 17, CERA-20C mean wave periods after calibration agree well with the buoy mean wave periods at Bozcaada especially for the longer wave periods. At

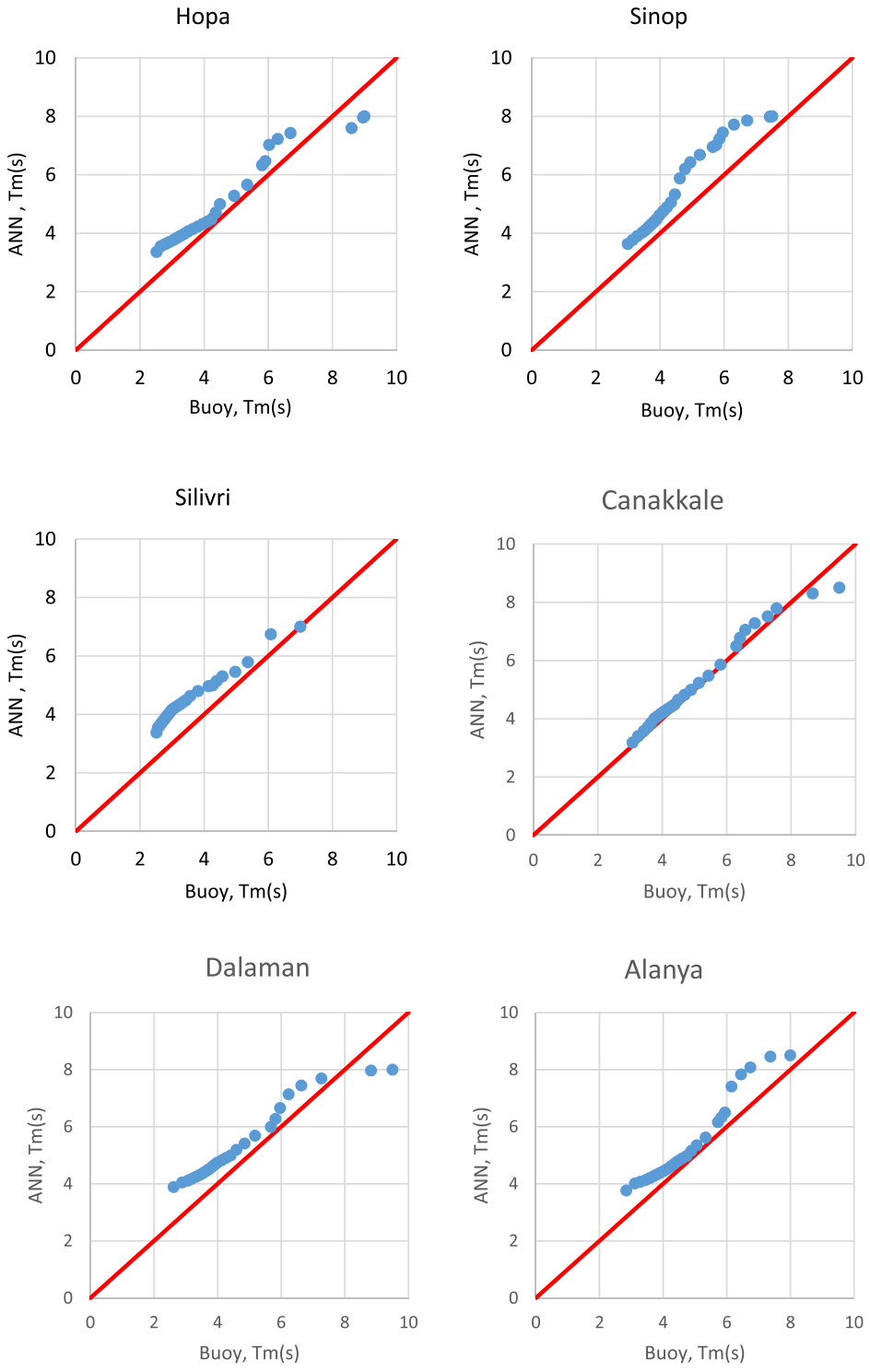

Fig. 15. Q-Q plots for ANN-computed altimeter Tm versus buoy measurement.

low to medium range, CERA-20C slightly overestimates the mean wave periods.

6. Error assessment for the verification study

After CERA-20C significant wave height and the mean wave period data were calibrated, they were compared against buoy data for verification purposes. The results are presented in terms of Q-Q plots in Fig. 14 for Hs and in Fig. 17 for Tm. The Q-Q plots indicate that the distributions of the CERA-20C wave height and mean period compare very well with their in-situ counterparts. In order to estimate the improvements introduced by the calibration, the error measures for Hs are calculated using both time

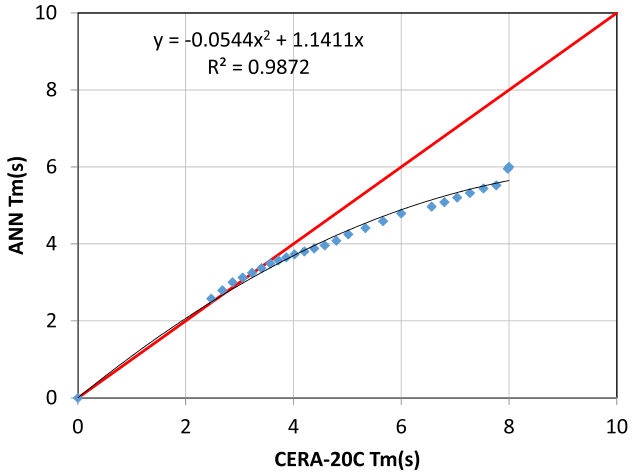

Fig. 16. Q-Q plot of altimeter (ANN) and CERA-20C mean wave periods at Bozcaada. The regression relation between the two and the square of the correlation coefficient are also shown.

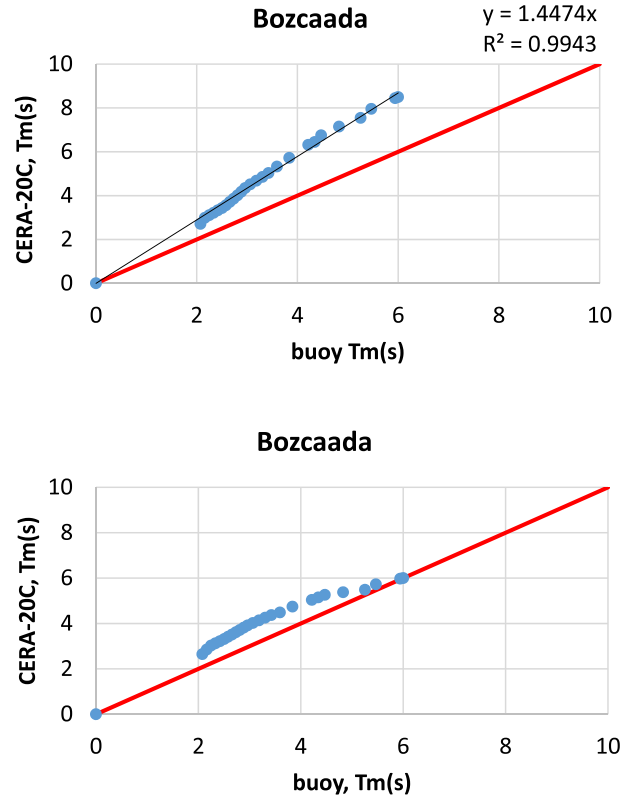

Fig. 17. Q-Q plots of CERA-20C Tm versus those of the buoy at Bozcaada before (upper panel) and after (lower panel) the calibration using altimeter ANN-derived wave periods.

series (one to one) comparison and Q-Q analysis. Statistical error measures of RMSE (root mean square error), SI (scatter Index = RMSE/mean value of the Hs of the buoy), bias, symmetric slope, A (defined as y = A x) and the correlation coefficient, R, are calculated before and after the calibration. Results of time series comparison are presented together with the mean values of the CERA-20C and the buoy significant wave heights in Table 8.

Table 8 shows that error in the time series comparison decreases slightly after the calibration of CERA-20C Hs data for Sinop, Hopa and Bozcaada. However, for Dalaman and Alanya the calibration did not reduce the errors. This result is not against any of the expectations since the calibration was performed by using Q-Q plots considering the importance of the highest sea states in the extreme wave analysis ignoring the exact time and the exact place of the occurrence of extreme waves.

The same statistical error measures were also calculated for Q-Q Hs data before and after the calibration. Table 9 displays the results of those error measures. Table 9 clearly indicates that the errors decrease after the calibration. Moreover, the symmetric slope, A, becomes closer to 1.0 (the ideal value).

Similar error measure calculations were performed on the mean wave period, Tm, data. CERA-20C Tm data were compared against their buoy counterparts at Bozcaada by using time series and Q-Q analysis. Results are presented in Table 10. It is clear from Table 10 that the errors decreased after calibration and there is a better agreement between the mean wave period data of the CERA-20C and the buoy measurements after CERA-20C period was calibrated using the altimeter ANN Tm estimations.

7. Conclusions

The century-long ocean wave data of European Centre for Medium-Range Weather Forecasts (ECMWF) were calibrated and verified by using satellite radar altimeter and in-situ measurements. The calibrated dataset will be used in the future for the calculation of the design waves with various return periods along the Turkish coasts. As a result, the following conclusions are derived:

Two 20th century re-analysis datasets of ECMWF (ERA-20C and CERA-20C) are compared. Both of the datasets give similar results. However, the coupled CERA-20C dataset is found to be slightly better in terms of statistical error measures for the significant wave height.

The comparison between the significant wave height and the mean wave period data of CERA-20C and the buoy at five measurement locations along the Turkish coasts indicates that CERA-20C wave data should be calibrated before they can be used for the extreme wave analysis.

Satellite radar altimeter, RA, data were found appropriate to be used for the calibration since RA and buoy Hs measurements are in very good agreement in terms of the quantiles (i.e. similar distributions). In addition to the satellite data, ERA5, which is the newest re-analysis dataset of ECMWF produced within the framework of European Union Copernicus Climate Change Service (C3S), was used as a second reference for the calibration of CERA-20C. After an extensive inter-calibration and combination procedure, the satellite Hs

Table 8
Statistical error measures for significant wave height, Hs, calculated using the one-to-one comparison between CERA-20C and the buoy measurements before (original) and after the calibration (calibrated) of CERA-20C Hs data.

Location	CERA-20C Hs data	RMSE	SI	bias	A	R	Mean of CERA-20C	Mean of buoy
Sinop	Original	0.4927	0.5662	0.2884	0.6064	0.7231	0.5818	0.8702
	Calibrated	0.4401	0.5057	−0.0674	0.9772	0.7231	0.9376	0.8702
Hopa	Original	0.4361	0.6961	0.2080	0.5625	0.8283	0.4185	0.6265
	Calibrated	0.3653	0.5831	−0.1042	0.9820	0.8283	0.7306	0.6265
Bozcaada	Original	0.6218	1.1850	−0.2509	1.2500	0.5200	0.7756	0.5247
	Calibrated	0.4556	0.8683	−0.0631	0.9472	0.5200	0.5878	0.5247
Dalaman	Original	0.3555	0.6247	−0.1190	0.9587	0.7669	0.6881	0.5691
	Calibrated	0.6224	1.0936	−0.4565	1.4290	0.7669	1.0256	0.5691
Alanya	Original	0.3143	0.5402	0.0764	0.7058	0.7768	0.5054	0.5819
	Calibrated	0.4107	0.7491	−0.2060	1.1677	0.7768	0.7879	0.5819

Table 9
Statistical error measures for significant wave height, Hs, calculated using Q-Q of CERA-20C and the buoy measurements before (original) and after the calibration (calibrated) of CERA-20C Hs data.

Location	CERA-20C Hs data	RMSE	A	R
Sinop	Original	0.63678	0.65412	0.99881
	Calibrated	0.16842	1.08192	0.99872
Hopa	Original	0.75602	0.61044	0.99007
	Calibrated	0.22041	0.97761	0.98917
Bozcaada	Original	0.71179	1.54403	0.99662
	Calibrated	0.24445	1.18092	0.99799
Dalaman	Original	0.71179	0.75048	0.96527
	Calibrated	0.43602	1.06198	0.98855
Alanya	Original	0.30452	1.23650	0.99437
	Calibrated	0.22180	1.09725	0.99704

data with a total duration of 18 years (1995–2012) for Envisat family and 26 years (1992–2017) for Jason family were obtained to calibrate CERA-20C significant wave height data.

In order to estimate the wave period from satellite RA measurements (Ku-band Hs together with Ku- and C-band backscatters), an Artificial Neural Networks (ANN) method was used. High correlations and lower errors in the test results of designed ANN model showed that mean wave period can be estimated from altimeter measurements for the enclosed seas providing that the ANN model is trained using enclosed sea data. ANN estimates of the mean wave periods were used to calibrate the CERA-20C mean wave periods.

The combined inter-calibrated altimeter datasets were prepared. They were used to calibrate CERA-20C significant wave height and mean wave period. Although the calibrated CER-20C datasets do not agree very well with the in-situ measurements based on the time series comparison, they show very good agreement when the distributions are compared (i.e. in terms of quantile–quantile, Q-Q, comparison). In fact Q-Q analysis shows that the largest sea states can be captured by CERA-20C data after calibration. Since the purpose of the study to derive wave datasets to be used in the extreme wave analysis, it is concluded that the calibrated CERA-20C wave data become appropriate for the extreme wave analysis in order to determine the design waves along the Turkish coasts in a future study. Moreover, the calibration method by using the extended and inter-calibrated datasets of combined altimeters can be applied to other sites around the world.

Acknowledgements

We would like to thank European Centre for Medium-Range Weather Forecasts (ECMWF) for making ERA-20C, CERA-20C and ERA5 wave data available. ERA5 is produced with the framework of the EU Copernicus Climate Change Service, C3S. Gratitude is also due to Prof. Dr. Erdal Özhan who was the director of the NATO TU-WAVES Project for providing the buoy data at Hopa, Sinop, Bozcaada, Dalaman and Alanya, and to the Turkish State Meteorological Organization for providing the buoy data at Bogaz, Silivri, Çanakkale, Antalya and Silifke.

This work was supported by Turkish Research Council, TUBITAK under the Grant: 117M968.

Table 10
Statistical error measures for the mean wave period, Tm, calculated using both one-to-one and Q-Q comparisons of CERA-20C and the buoy measurements at Bozcaada before (original) and after the calibration (calibrated) of CERA-20C Tm data.

Comparison type	CERA-20C Tm data	RMSE	A	R	SI	Bias	CERA-20C Mean Tm(s)	Buoy Mean Tm(s)
Time series	Original	1.5163	1.3419	0.3643	0.5169	−1.1081	4.0416	2.9335
	Calibrated	1.0551	1.2072	0.3510	0.3597	−0.7266	3.6602	2.9335
Q-Q	Original	1.6632	1.4474	0.9974				
	Calibrated	0.7793	1.1691	0.9736				

References

Abdalla, S., Janssen, P.A.E.M., 2018. Monitoring waves and surface winds by satellite altimetry; applications. CRC Press, Taylor & Francis Group, USA, pp. 381–425.

Abdalla, S., Janssen, P.A.E.M., Bidlot, J.-R., 2011. Altimeter near real time wind and wave products: Random error estimation. Mar. Geod. 34 (3–4), 393–406.

Abdalla, S., 2013. Wind and wave data selection for climate studies in enclosed seas. In: Proceedings of the 10th Global Congress on ICM: Lessons Learned to Address New Challenges, EMECS 2013 - MEDCOAST 2013 Joint Conference, Marmaris, Turkey, pp. 1347–1358.

Abdalla, S., Yilmaz, N., 2015. Suitability of ECMWF ERA-20C for wind and wave climate in the Black Sea. In: Proceedings of the 12th International Conference on the Mediterranean Coastal Environment, MEDCOAST 2015, Varna-Bulgaria, pp. 745–756.

Badulin, S.I., 2014. A physical model of sea wave period from altimeter data. J. Geophys. Res. Oceans 119 (2), 856–869.

Dada, O.A., Li, G., Qiao, L., Ma, Y., Ding, D., Xu, J., Yang, J., 2016. Response of waves and coastline evolution to climate variability off the Niger Delta coast during the past 110 years. J. Mar. Syst. 160, 64–80. https://doi.org/10.1016/j.jmarsys.2016.04.005.

Dafka, S., Xoplaki, E., Toreti, A., et al., 2016. The Etesians: from Observations to Reanalysis. Climate Dynamics 47 (5–6), 1569–1585.

Dee, D.P., Uppala, S.M., Simmons, A.J., Berrisford, P., Poli, P., Kobayashi, S., Vitart, F., 2011. The ERA-Interim reanalysis: Configuration and performance of the data assimilation system. Q. J. R. Meteorolog. Soc. 137 (656), 553–597. https://doi.org/10.1002/qj.828.

ECMWF. (n.d.). ERA 5. Retrieved from https://www.ecmwf.int/en/forecasts/datasets/reanalysis-datasets/era5.

Gommenginger, C.P., Srokosz, M.A., Challenor, P.G., Cotton, P.D., 2003. Measuring ocean wave period with satellite altimeters: A simple empirical model. Geophys. Res. Lett. 30 (22), 2150. https://doi.org/10.1029/2003GL017743.

Hersbach, H., Bell, B., Berrisford, P., Hirahara, S., Horanyi, A., Thepaut, J.N., 2020. The ERA5 global reanalysis. Quarterly J. Royal Meteorological Soc. (in review) Submitted for publication.

Laloyaux, P., de Boisséson, E., Dahlgren, P., 2017. CERA-20C: An Earth system approach to climate reanalysis. ECMWF Newsletter No. 150, 25–30.

Janssen, P.A.E.M., Abdalla, S., Hersbach, H., Bidlot, J.R., 2007. Error estimation of buoy, satellite, and model wave height data. J. Atmos. Oceanic Technol 24, 1665–1677.

Kumar, P., Min, S.K., Weller, E., Lee, H., Wang, X.L., 2016. Influence of climate variability on extreme ocean surface wave heights assessed from ERA-interim and ERA-20C. J. Clim. 29 (11), 4031–4046. https://doi.org/10.1175/JCLI-D-15-0580.1.

Mackay, E.B.L., Retzler, C.H., Challenor, P.G., Gommenginger, C.P., 2008. A parametric model for ocean wave period from Ku band altimeter data. J. Geophys. Res. Oceans 113 (C3), C03029. https://doi.org/10.1029/2007JC004438.

Ozbahceci, B.O., 2020. Extreme value statistics of wind speed and wave height of the Marmara Sea based on combined radar altimeter data. Adv. Space Res. 66 (10), 2302–2318. https://doi.org/10.1016/j.asr.2019.08.025.

Özhan, E., Abdalla, S., 1999. Wind and wave climatology of Turkish coasts and the Black Sea: An overview of the NATO TU_WAVES project. In: Proceedings of the International MEDCOAST Conference on Wind and Wave Climate of the Mediterranean and the Black Sea, 1–20. Antalya, Turkey.

Özhan, E., Abdalla, S., 2002. Wind and Deep Water Wave Atlas along the Turkish Coasts. TMK/MEDCOAST Publications, Ankara.

Patra, A., Bhaskaran, P.K., 2017. Temporal variability in wind–wave climate and its validation with ESSO-NIOT wave atlas for the head Bay of Bengal. Clim. Dyn. 49 (4), 1271–1288. https://doi.org/10.1007/s00382-016-3385-z.

Poli, P., Hersbach, H., Dee, D.P., Berrisford, P., Simmons, A.J., Vitart, F., Fisher, M., 2016. ERA-20C: An atmospheric reanalysis of the twentieth century. J. Clim. 29 (11), 4083–4097. https://doi.org/10.1175/JCLI-D-15-0556.1.

Quilfen, Y., Chapron, B., Collard, F., Serre, M., 2004. Calibration/validation of an altimeter wave period model and application to TOPEX/Poseidon and Jason-1 altimeters. Mar. Geod. 27 (3–4), 535–549. https://doi.org/10.1080/01490410490902025.

Scharroo, R., Leuliette, E.W., Lillibridge, J.L., Byrne, D., Naeije, M.C., Mitchum, G.T., 2013. RADS: Consistent multi-mission products. In: Proc. of the Symposium on 20 Years of Progress in Radar Altimetry, Venice, 20-28 September 2012, Eur. Space Agency Spec. Publ., ESA SP-710, p. 4 pp.

Stopa, J.E., 2018. Wind forcing calibration and wave hindcast comparison using multiple reanalysis and merged satellite wind datasets. Ocean Model. 127, 55–69. https://doi.org/10.1016/j.ocemod.2018.04.008.

Tayfur, G., 2012. Soft Computing in Water Resources Engineering. WIT Press, Southampton, UK.

Vinoth, J., Young, I.R., 2011. Global estimates of extreme wind speed and wave height. J. Climate 24 (6), 1647–1665.

Young, I.R., Zieger, S., Babanin, A.V., 2011. Global trends in wind speed and wave height. Science 332 (6028), 451–455. https://doi.org/10.1126/science.1197219.

Young, I.R., Sanina, E., 2017. Calibration and cross validation of a global wind and wave database of altimeter, radiometer, and scatterometer measurements. J. Atmos. Oceanic Technol. 34, 1285–1306. https://doi.org/10.1175/jtech-d-16-0145.1.